Theoretical and Applied Climatology (2019) 136:1435–1451
https://doi.org/10.1007/s00704-018-2569-3

ORIGINAL PAPER

The analysis of global surface temperature wavelets from 1884 to 2014

Carlos Batista Silva[1] · Maria Elisa Siqueira Silva[1] · Nísia Krusche[2] · Tércio Ambrizzi[3] · Nelson de Jesus Ferreira[4] · Pedro Leite da Silva Dias[3]

Received: 13 June 2017 / Accepted: 18 July 2018 / Published online: 28 July 2018

Abstract

In this paper, we sought to investigate the spatial and temporal variability of the global sea surface temperature in the 1884–2014 period, through wavelet analysis. Results for tropical, subtropical, and extratropical areas indicate important oscillations in the 1–12-month and 1–2-, 2–4-, 4–8-, and 8–12-year spectral ranges, as obtained in other studies which used regional mean SST values instead of global gridpoint data with 2.5° resolution, as used in this study. The intraseasonal (1–12 months) and interannual (1–2 years) oscillations are much more evident in the tropical latitudes. On the other hand, lower frequency oscillations (2–4, 4–8, and 8–12 years) are more dominant away from tropical regions. The faster oscillation scale (1–12-month and 1–2- and 2–4-year spectral ranges) SST variance presents negative trends throughout the entire period, while the values associated with the slower oscillation scales (4–8- and 8–12-year spectral ranges) present increasing trends. The reversal of trends for distinct SST spectral ranges over the whole period suggests energy exchanges between distinct oscillatory phenomena. In addition, the energy increase of slower frequencies suggests the prolonged settlement of low-frequency climatic patterns in the future, providing more inertial climatic patterns. The strongest diminishing values of SST variance associated with the higher frequency oscillations were observed in the Atlantic oceanic basins. The strongest increasing values for the lower oscillations, mainly related to the 2–4- and 4–8-year spectral ranges, were observed in the Pacific basins. In general, the Pacific basins are closely correlated with the global mean ($0.55 \le r \le 0.92$), compared with the Atlantic ($0.31 \le r \le 0.75$) and Indian ($0.12 \le r \le 0.56$) basins.

1 Introduction

Intraseasonal, interannual, and decadal variabilities are important scales used to characterize climatic phenomena and they are frequently studied through spectral analysis. In this study, we seek to understand the global distribution of sea surface temperature mainly in interannual and decadal spectral bands through wavelet analysis. Considering multiple variables, spectral analysis allows us to construct connections between them and, thus, connections between distinct phenomena. Besides Fourier analysis, wavelet transform has been used in many studies in atmospheric sciences as a way to discover the temporal variation of associated spectral energy (e.g., Farge 1992; Weng and Lau 1994; Lau and Weng 1995; Mak 1995; Gu and Philander 1995; Torrence and Compo 1998; Torrence and Webster 1999; An and Wang 2000; Minobe et al. 2002; Newman et al. 2003; Kayano and Andreoli 2004; Andreoli and Kayano 2004; Janicke et al. 2009), which is important in

✉ Carlos Batista Silva
krlosbatist@gmail.com

✉ Maria Elisa Siqueira Silva
mariaelisa.siqueirasilva@gmail.com

✉ Nísia Krusche
nkrusche.furg@gmail.com

✉ Tércio Ambrizzi
ambrizzi@model.iag.usp.br

✉ Nelson de Jesus Ferreira
nelson.ferreira@cptec.inpe.br

✉ Pedro Leite da Silva Dias
pedro.dias@iag.usp.br

[1] Department of Geography, College of Philosophy, Letters and Human Sciences, University of São Paulo, São Paulo, Brazil

[2] Center for Computational Sciences, Federal University of Rio Grande, Rio Grande, Brazil

[3] Department of Atmospheric Sciences Institute of Astronomy, Geophysics and Atmospheric Sciences, University of São Paulo, São Paulo, Brazil

[4] National Institute of Space Research—INPE, São José dos Campos, Brazil

atmospheric studies, considering their dynamical character. The temporal variability of specific frequencies constitutes the most important aspect of wavelet analysis. The understanding of temporal variation of particular frequencies is especially important for climatic studies, as pointed out by many authors, e.g., Torrence and Compo (1998), Whitcher et al. (2000), Vitorino et al. (2006), Minobe et al. (2002), Kayano and Andreoli (2004), and Andreoli and Kayano (2004). Besides the spectral variation in time, Torrence and Webster (1999) indicate another advantage of the wavelet technique referring to the study of phase change for nonstationary variables. They analyzed interdecadal changes in the El Niño/Southern Oscillation (ENSO)-Indian Monsoon in the last 125 years. Oscillations of 2–7 years, classified as higher frequency, were identified during the 1875–1920 and 1960–1990 periods, while oscillations of lower frequency were identified in the 1920–1960 period. The wavelet application to atmospheric and climatic studies considers single time series without taking into account the spatial dimension, as shown in the studies carried out by Farge (1992), Lau and Weng (1995), Mak (1995), Kumar and Foufoula-Georgoiu (1997), Torrence and Webster (1999), An and Wang (2000), Kayano and Andreoli (2004), Andreoli and Kayano (2004), and Vitorino et al. (2006).

An and Wang (2000) identified changes in the dominant ENSO scale oscillation with SST data in the Niño 3.4 region: varying from 2 to 4 years, in the period 1962–1975, to 4–6 years, in the following 1980–1993 period. The authors argue that the energy exchange from higher to lower frequencies suggests a significant change in the ENSO structure.

Kayano and Andreoli (2004) investigated the link between the Northeastern Brazil precipitation, north and south equatorial Atlantic SST, and the sea level pressure from the North Atlantic Oscillation region, in decadal scale (9–12 years), for the period 1871–1991, through wavelet and partial correlation analysis. The authors concluded that the decadal precipitation variability over Northeast Brazil can be associated with the Pacific Decadal Oscillation (PDO) and the North Atlantic Oscillation (NAO) (both decadal oscillations).

In order to investigate the spatial behavior of submonthly and intraseasonal convection variability over South America and adjacent areas, Vitorino et al. (2006) applied wavelet transform to longwave radiation and relative vorticity data for the 1979–1996 period and indicated the intraseasonal scale prevalence for tropical convective processes, observing important oscillations for the 7–15-day scale, associating them with extratropical convection during spring and winter, and also with greater energetic intensity during spring and winter in tropical areas while subtropical and extratropical areas presented higher energy during winter and autumn.

Although several studies have been made in the last decades to identify important spectral ranges associated with climatic behavior, as previously mentioned, they did not give detailed attention to the spatial distribution over the globe obtained from this technique and its respective temporal evolution. Accordingly, and with recognition of the importance of ocean variability in the climate characterization (Walker and Bliss 1932; Troup 1965; Bjerknes 1969; Horel and Wallace 1981; Karoly 1989), it is proposed here to analyze the temporal and spatial distribution of global sea surface temperature spectral energy between 1884 and 2014, obtained from wavelet transform. This analysis allows the identification of the possible trends and climatic variability of phenomena on distinct scales, both globally and regionally, in the oceanic basins.

2 Data and methods

The wavelet transform is applied to monthly SST data, for the period 1854–2014, globally distributed. SST data with 2.0° of spatial resolution were acquired from the System Research Laboratory—ESRL, NOAA (http://www.esrl.noaa.gov/psd/data/gridded/data.noaa.ersst.html). A full description of NOAA's SST dataset characteristics is given in Kaplan et al. (1998). The use of wavelet analysis was motivated by the interest in the analysis of distinct spectral ranges (Flandrin 1988; Weng and Lau 1994; Torrence and Compo 1998; Setoh et al. 1999), particularly for SST data, and taking on the nonstationary climate characteristic. Before applying the wavelet transform to SST monthly data, the linear trend and seasonality were removed from the SST time series. The seasonality was removed by removal of the climatological monthly mean, keeping just the interannual variability of the annual cycle.

The wavelet transform is a mathematical technique used in the detection of temporal structure of multiscale variations, into a specific finite and nonstationary data time series (Lau and Weng 1995). This technique has the property of transforming a one-dimensional into a two-dimensional time series, in the time-frequency domain, allowing for the observation of dominant oscillation modes in time. The main wavelet functions are composed of small waves generated by dilatation (a) and translations (b) of a simple function $\psi(t)$. The wavelet transform can be represented by different functions: Morlet, Paul, Dog (Torrence and Compo 1998), Haar (Weng and Lau 1994), Meyer (Mak 1995), and Daubechies (Daubechies 1990), among others. The Morlet function was used here (Morlet 1983). This wave is modulated by a Gaussian envelope, $\psi(t) = e^{iw_0\eta}e^{\frac{-\eta^2}{2}}$, where $\eta = t/s$, t is time, s the wavelet scale, and w_0 the nondimensional frequency. The wavelet transform in each scale is normalized by $s^{-1/2}$ allowing the comparisons between the results. The wavelet variance or the associated energy is given by $E = [\psi_{\alpha,\,b}]^2$.

The results shown constitute the absolute values of SST variance (or, in other times, its respective temporal anomaly)

for each spectral range. The first 360 months was removed from the results in order to avoid secondary effects of the Morlet function decay (Weng and Lau 1994; Kaplan et al. 1998; Vitorino et al. 2006). Additionally, the reconstructed SST data from 1856 to 1900 presents very high standard deviation in relation to the rest of the time series, as indicated by Kaplan et al. (1998), which was another reason for eliminating the initial period.

The resulting analyses were made for specific spectral ranges: 1–12 months, 1–2 years, 2–4 years, 4–8 years, and 8–12 years. These ranges were selected based on initial spectral tests for specific oceanic areas, tropical (23.5° N–23.5° S), subtropical (23.5° N–66.3° N; 23.5° S–66.3° S), and extratropical (66.33° N–90.0° N; 66.3° S–90.0° S) latitudes, both for the Southern and Northern Hemispheres, for distinct ocean basins. The scientific literature (Torrence and Compo 1998; Torrence and Webster 1999; Setoh et al. 1999; Kayano and Andreoli 2004; Andreoli and Kayano 2004) also corroborates the selection of the specific spectral ranges adopted here. Animation of global SST variance during the selected period allows us to depict the more significant areas for each spectral range. The videos can be accessed at the link http://krlosbatist.wixsite.com/meusite.

The wavelet transform was separately applied to each grid point, and the resulting variance was then spatially analyzed, allowing for the evaluation of the spatial-temporal evolution. The software used for the SST variance computation (written in Fortran) is based on that developed by Torrence and Compo (1998) and can be found at http://paos.colorado.edu/research/wavelets/. We adjusted the program to compute the spectral variance for a spatial matrix instead of one single time series. The results were obtained for the spectral ranges previously defined for three distinct spatial domains: global, hemispheric, and specific oceanic basins, North Atlantic (75° W–10° E and 0–90° N), South Atlantic (70° W–20° E and 0–90° S), North Pacific (80° W–120° E and 0–90° N), South Pacific (80° W–140° E and 0–90° S), and Indian basin (40° E–120° E and 20° N–90° S). In general, all SST variance values are presented as anomalies in relation to the whole period (1884–2014) just to make visualization easier. Additionally, the SST variance trend during the whole period for each spectral range was analyzed to verify a possible energy transference between phenomena of different scales. A statistical significance test was applied to the energy values as suggested by Torrence and Compo (1998).

3 Results and discussion

The results are displayed in two distinct sections. Section 3.1 presents the global spectral behavior for large oceanic areas (tropical, subtropical, and extratropical) in order to show the more significant spectral ranges. Section 3.2 shows the time evolution of the SST variance globally averaged, for each hemisphere and for each oceanic basin, as described in the previous section.

3.1 Global SST spectral variance for tropical, subtropical, and extratropical areas

Spectral power and the respective SST variance (wavelet results) applied to tropical, subtropical, and extratropical areas, for the 1854–2014 period, are displayed in Fig. 1. In general, tropical and subtropical areas (Fig. 1(a–d)), both in the Southern and Northern Hemispheres, show higher energy for lower frequencies (oscillations of 4 years or more), while extratropical areas (Fig. 1(e, f)) show important high energy for higher frequencies (oscillations with periodicities between 1 and 2 years). This aspect is also seen in the temporal SST variance graphics (left side in Fig. 1). Tropical Northern Hemisphere SST shows strong energy for the 8–16 spectral range (Fig. 1(b_2)), which is not observed in the Southern Hemisphere (Fig. 1(a_2)).

El Niño-South Oscillation (ENSO), Indian Oscillation Dipole (IOD), Indian Ocean basin-wide (IOBW), and the Tropical Atlantic Meridional Gradient constitute well-known tropical variability modes and are examples of climatic phenomena associated with the results shown in Fig. 1(a, b). The ENSO, since the beginning of the 1980s, has been classified as very low-frequency phenomena (characterized by oscillations of 4–6 and 4–7 years), whereas in previous periods, such as in 1963–1975, the ENSO showed a higher frequency, with a characteristic oscillation period between 2 and 4 years, as mentioned by An and Wang (2000). The IOD is an interannual variability mode, with a period of between 2 and 5 years (Saji et al. 1999; Webster et al. 1999; Yamagata et al. 2003) characterized by nonperiodic Indian SST oscillations, presenting positive and negative phases (Saji et al. 1999). The intense warming of tropical waters in the Indian Ocean, with a maximum temperature peak in the beginning of springtime, known as IOBW, is characterized by a 3-year oscillation (Chu et al. 2014). Saji and Yamagata (2003) and Latif and Barnett (1995) raise the question about the ENSO participation as crucial factor for the IOBW occurrence, showing an apparent interconnection between tropical physical modes of different frequency scales. The Tropical Atlantic Meridional Gradient is commonly associated with decadal (~ 10 years) (Carton et al. 1996; Wagner 1996; Kayano and Andreoli 2004) and interannual (2–5 years) (Carton et al. 1996) SST variabilities and is responsible for wet and dry periods in the north of South America and the Caribbean (Nobre and Shukla 1996). The contributions by Wagner (1996) illustrate the prominent decadal scale control mechanism in the building up of the tropical meridional gradient. The mentioned studies corroborate the main characteristics of the temporal variability represented in Fig. 1.

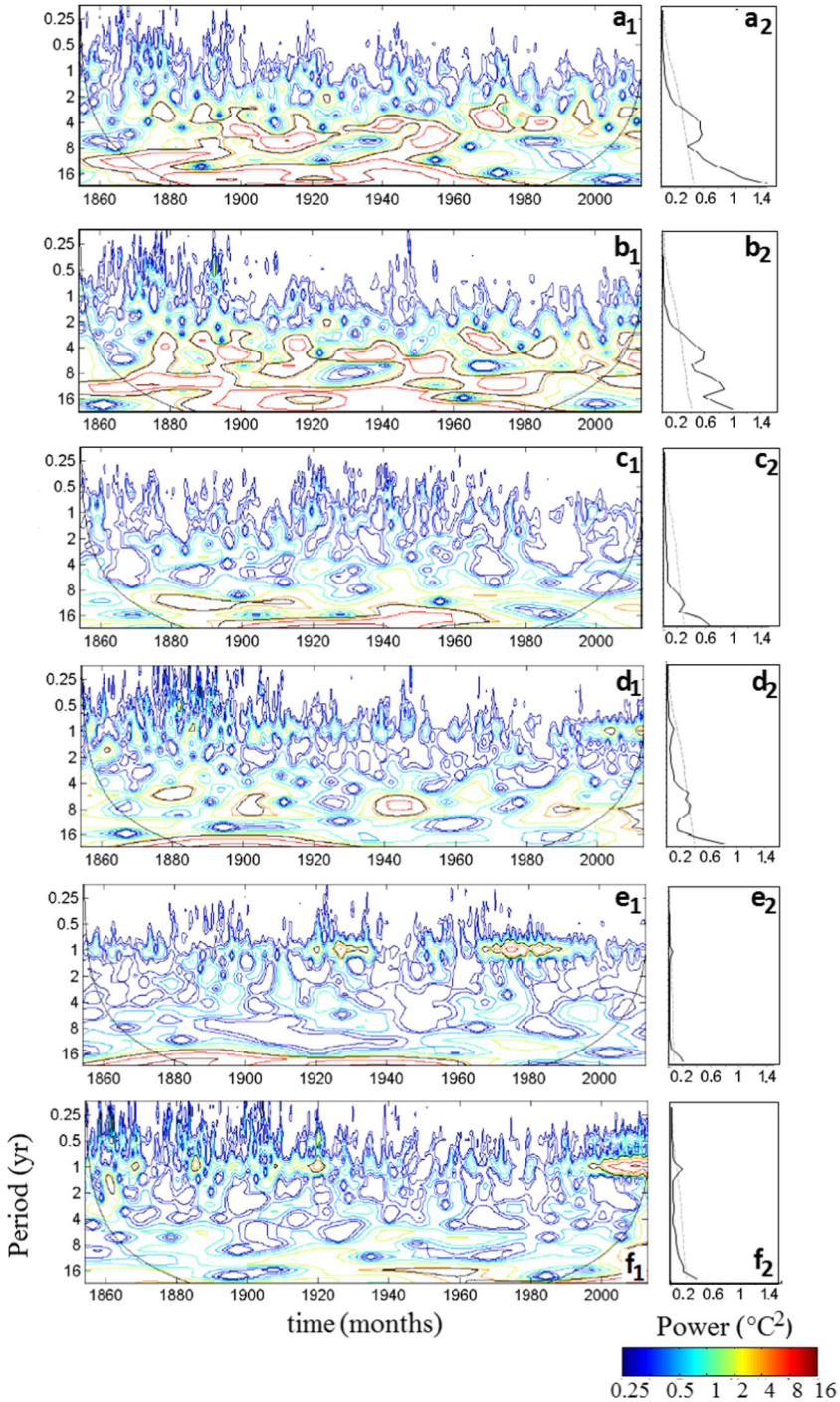

Fig. 1 (a_1) Wavelet and (a_2) total power spectra from tropical SST ($^oC^2$) South Hemisphere, for the 1854–2014 period; (b_1) and (b_2), the same as (a_1) and (a_2), but for tropical North Hemisphere; (c_1) and (c_2), the same as (a_1) and (a_2), but for subtropical South Hemisphere; (d_1) and (d_2), the same as (a_1) and (a_2), but for subtropical North Hemisphere; (e_1) and (e_2), the same as (a_1) and (a_2), but for extratropical South Hemisphere; and (f_1) and (f_2), the same as (a_1) and (a_2), but for extratropical North Hemisphere. Statistical significance ($p = 0.05$, Student's t test) is shown by black isolines in the left panels. Energy intensity is shown by colored isolines in the left panels from blue to red

In subtropical areas, both for the Northern and Southern Hemisphere (Fig. 1(c, d)), we verify less significant SST variance for spectral ranges of relatively higher frequencies compared with the variance in tropical areas for the same spectral ranges (Fig. 1(a, b)). In general, the most energetic spectral ranges in subtropical areas are those related to oscillations of 7–16 years, for the Southern Hemisphere, and 4–9 years, for the Northern Hemisphere. Oscillations with periodicities greater than 16 years, in both hemispheres, show high energy values which are not statistically significant.

Several studies have also documented the interdecadal climate fluctuations in the Pacific basin (Francis and Hare 1994; Hare and Francis 1995; Latif and Barnett 1994, 1996 and Zhang et al. 1997), highlighting the PDO, which is defined by the leading mode of empirical orthogonal function (EOF) applied to monthly anomalies of sea surface temperature in the Pacific Ocean poleward of 20° N (Davis 1976; Mantua et al. 1997). The PDO is characterized as a climatic mode of very low frequency with periodicities of 15–25 years (Mantua and Hare 2002). The positive PDO phase is characterized by

positive SST anomalies over the central-eastern Pacific, spread over the southwestern coast of North America, while the negative phase is characterized by the opposite spatial pattern (Mantua et al. 1997). Since 1901, the PDO has been characterized by two complete cycles: the positive phases constitute the periods 1925–1946 and 1977–1996, and the negative phases, the periods 1900–1924 and 1947–1976. From 1998 to 2014, negative PDO signs were more frequent (http://research.jisao.washington.edu/pdo/).

The extratropical areas of both hemispheres show more significant oscillations of around 1 year. Oscillations with a period longer than 16 years, though outside the influence cone, show a high SST variance values in extratropical regions (Latif and Barnett 1994, 1996; Hare and Francis 1995; Mantua et al. 1997; Minobe 1997; Zhang et al. 1997; Gershunov and Barnett 1998; Mantua and Hare 2002). Considering the results in the literature and the spectral ranges with the highest energy identified here, it was decided to investigate the behavior of the following spectral ranges: 1–12 months, 1–2 years, 2–4 years, 4–8 years, and 8–12 years.

3.2 Temporal evolution of global SST variance

The temporal evolution of global mean SST variance obtained for each spectral range, as indicated in Fig. 2, presents distinct averages and standard deviation (sd) values in the period 1884–2014. SST oscillations of 1–12 months and 1–2 years, classified here as high-frequency ranges, present the lowest amplitude values if compared with the remaining ranges. SST variance presents global standard deviation equal to 0.024 and 0.015, respectively, for the 1–12-month and 1–2-year ranges. The 2–4-, 4–8-, and 8–12-year ranges present greater standard deviation values, respectively, equal to 0.34, 0.04, and 0.034.

3.2.1 Oscillations of 1–12-month periods

SST variance values for the 1–12-month spectral range show continuous significant decreasing values during the period 1884–2014, while the SST variance for the 4–8- and 8–12-year spectral ranges shows increasing values. One possible question that arises has to do with the energy exchange between different scales. Raupp and Silva Dias (2006) showed energy exchanges between distinct waves forced by the geostrophic mode, based on resonant interactions between equatorial waves and the tropical diurnal heat source, suggesting that diurnal variations in tropical convection can play an important role in the low-frequency atmospheric circulation. More recently, Ramirez et al. (2017) developed a simplified multiscale atmosphere-ocean coupled model for the tropical

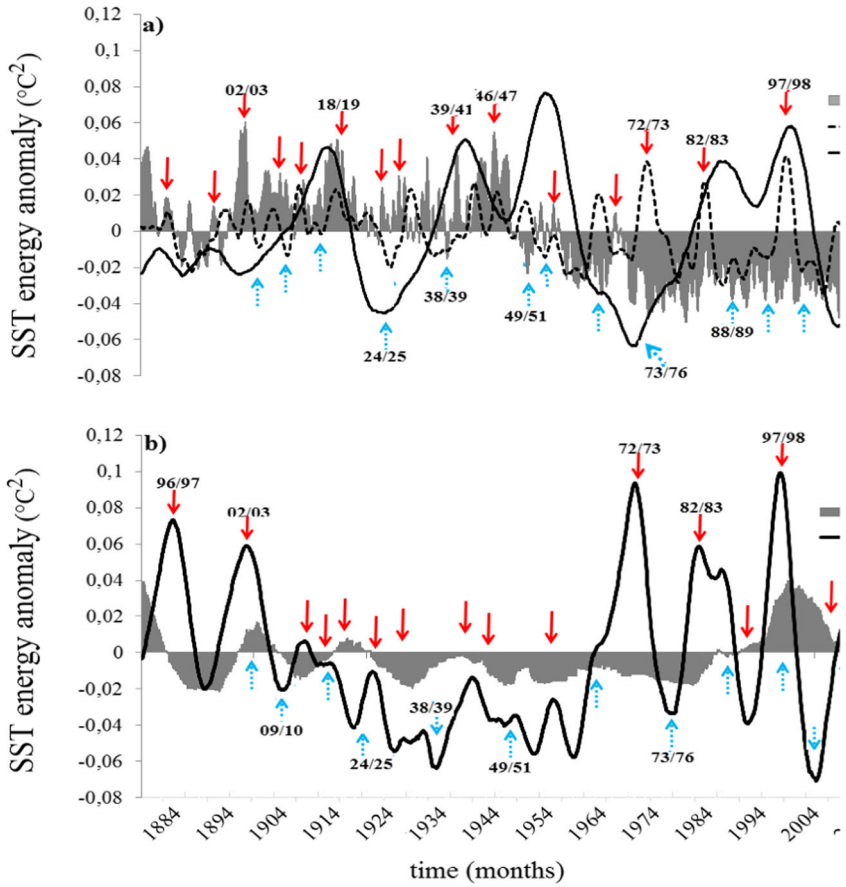

Fig. 2 Global mean SST variance (°C^2) between Jan, 1884 and Dec, 2014, for the spectral ranges **a** 1–12 months (gray bars), 1–2 years (dashed line), and 4–8 years (solid line) and **b** 2–4 years (solid line) and 8–12 years (gray bars). Values are normalized by standard deviation. Intense El Niño and La Niña events (Huang et al. 2015) are respectively marked by red and blue arrows

interactions between synoptic, intraseasonal, and interannual scales. This paper demonstrates that the intraseasonal timescale is connected to the fast equatorial synoptic and slow interannual timescales on the interannual and even longer timescales. These theoretical results support the present observational results ensuring a theoretical basis for the energy exchanges between distinct spectral ranges. Farge (1992) also discusses the energetic exchanges between higher and lower frequency oscillations though he concentrates on turbulent circulation. Therefore, considering the linear trends shown in Fig. 3 and looking to the future, oscillations with periodicities of 4–8- and 8–12-year ranges may be associated with more energy in a future climate.

Positive and negative SST variances are usually associated with the occurrence of El Niño (EN) and La Niña (LN) events, which are indicated by red and blue arrows, respectively, in Fig. 2. During the whole period, EN event occurrence (35%) is in general more closely associated with maximum SST variance (1–12-month spectral range) than LN (25%) which is associated with minimum SST variance. Among all the considered SST frequency ranges, the 1–2-year spectral range seems to provide the best adjustment to the EN and LN periodicity of the total number of registered EN and LN events with 62.5 and 35% of the events, respectively, occurring concomitantly with energy peaks and lows, between 1884 and 2014. The SST variance peaks and lows observed in the 1–12-month spectral range are also firmly associated with EN and LN events, showing similar percentages of 55 and 42%, respectively, as in the values reported by Huang et al. (2015). The peaks and lows observed in the 2–4-year spectral range SST variance show similar percentages to the EN and LN events of 37.5 and 18%, respectively. For all considered spectral ranges, LN occurrence is not closely associated with minimum values of the SST variance, though, in particular cases, such as in 1970 and 1988–1989, LN events can be closely associated with the minimum SST variance values, as seen in Fig. 2.

Considering all the oceanic basins together, the SST variance linear evolution for the 1–12-month spectral range shows a negative trend in the whole period, as seen in Fig. 3. Taking the oceanic basins separately, as shown in Fig. 4, the North and South Atlantic are the basins showing the strongest decrease in the period. The physical interpretation of the linear trend is that higher frequency (intraseasonal) oscillations have become less energetic during the analyzed period in all oceanic basins, with varying intensities.

The time evolution of the 1–12-month spectral range SST variance (Fig. 5) of the North Pacific and the North Atlantic basins is the most linearly associated with the global mean, with linear correlation values of 0.75 and 0.48 (Table 1), respectively. The South Pacific and the Indian basins show the lowest linear correlation values for the 1–12-month spectral range (0.55 and 0.56, respectively), probably resulting in their lower strength in the global mean for this spectral range.

Differently from the energy in other basins, the North Pacific and South Atlantic energy related to the 1–12-month spectral range increases during the first half of the total period and decreases, like the remaining basins, in the second half, as seen in Fig. 6. The linear correlation increases between the global SST variance for the 1–12-month spectral range and the respective values for the Indian and the South Atlantic basin, from the first to the second halves of the time series, indicating that these specific basins may be becoming more associated with the North Pacific oscillations and also that the North and the South Pacific are becoming more influential in terms of global energy.

3.2.2 Oscillations of 1–2-year periods

Considering the SST variance for the 1–2-year spectral range, both the North and the South Pacific are the oceanic basins which are mostly linearly associated with the global mean, with correlation values equal to 0.73 and 0.79, respectively, as shown in Table 2. The remaining oceanic basins present

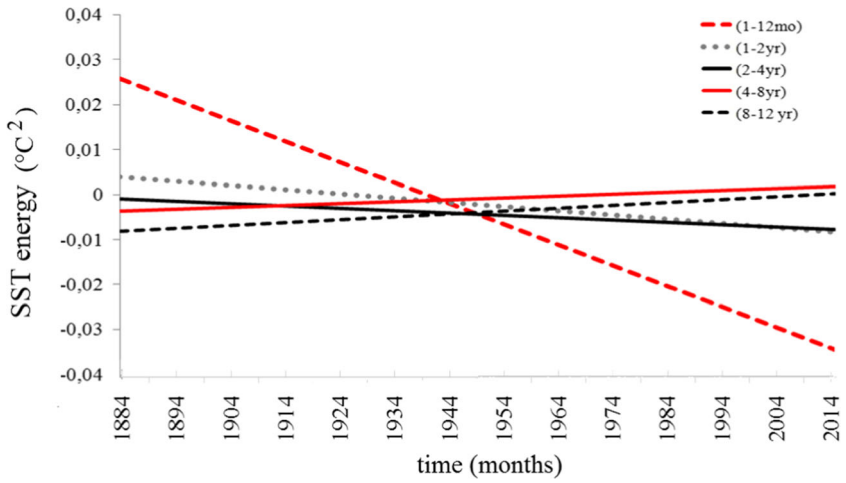

Fig. 3 Global mean SST variance linear trends during 1884–2014 for the spectral ranges: 1–12 months (dashed red line), 1–2 years (dotted gray line), 2–4 years (continuous black line), 4–8 years (continuous red line), and 8–12 years (black dashed line)

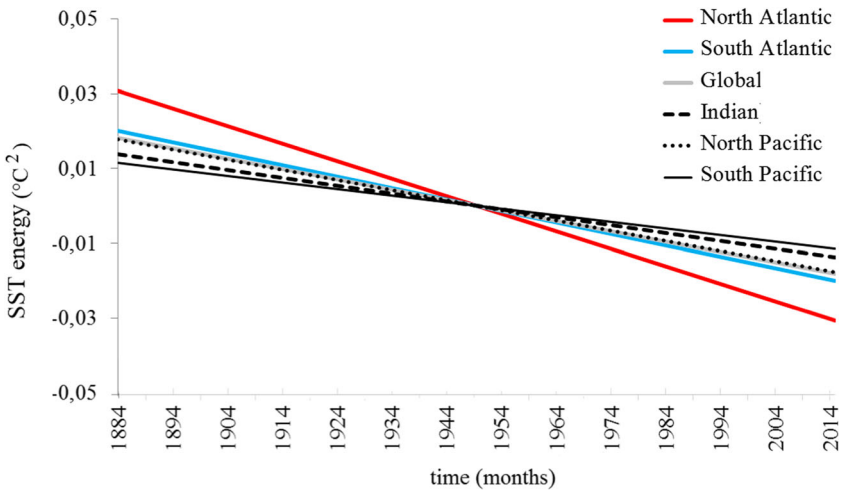

Fig. 4 Linear trend of SST variance for the 1–12-month spectral range for the global mean (gray): Indian (dashed black), North Atlantic (red continuous), North Pacific (dotted black), South Atlantic (blue continuous), and South Pacific (black continuous) oceanic basins, in the 1884–2014 period. Statistical significance (Student's *t* test) is higher than 99% in all cases

very low correlation values ($|r| < 0.16$) in relation to the global mean for oscillations of 1–2 years. This aspect (Table 2) can also be seen through Fig. 7 (by the continuous and dotted black lines representing the South and the North Pacific, respectively). In other words, the Pacific Ocean oscillations of 1–2-year period are much more important globally in relation to the other oceanic basins, at least in a linear approach.

Focusing on ENSO events, the North and South Pacific 1–2-year spectral range oscillations show high linear correlation with global mean values during EN periods, as seen in Fig. 7, which should be, at a certain level, an expected result once we are dealing with 1–2-year oscillations that are in agreement with the scientific literature of ENSO variability (Rasmusson et al. 1990). In order to measure the concomitance between any ENSO event and the spectral energy from the oceanic basins, linear correlation computation was taken for specific periods. Particularly, the 1965–1966 EN event shows high correlation with almost all oceanic basins, except in the South Atlantic, suggesting global teleconnection between the basins, though its intensity was classified as moderate. The 1972–1973 and 1982–193 EN events show higher correlation values with the North Pacific, South Pacific, and South Atlantic, and the 1997–1998 EN events show higher correlation values only with the North and South Pacific (Table 3). The LN 1970–1971 period shows high correlation values with all oceanic basins except the South Atlantic, and the 1988–1989 LN event shows high correlation values only with the South Atlantic. The specific periods selected here such as El Niño (1972/1973, 1982/1983, and 1997/1998) were classified as strong events (Jin et al. 2001, 2003; An and Jin 2004; Wang and Picaut 2004; Okumura and Deser 2010).

EN and LN events are associated with high and low SST spectral energy considering the increasing values of SST variance for lower frequency oscillations (4–8- and 8–12-year spectral ranges) and its decreasing for higher frequency oscillations (1–12-month and 1–2- and 2–4-year spectral ranges) over the total period of 1884–2014, as shown in Fig. 3 (as also shown in Tables 1, 2, and 4). The years 1965, 1973, 1983, and 1997, characterized by strong EN events, are marked by high SST energy values in the 1–2-year spectral ranges, as seen in Fig. 7. On the other hand, the 1970–1971 periods and 1988–1989, characterized by LN events, have minimum SST energy values. From the 23 ENSO events observed between 1950 and 2010, defined by the Oceanic Niño Index—ONI, 11 are associated with the 1–2- and 2–4-year spectral energy, seven are associated with the 1–12-month spectral range, and five are more associated with 4–8-year spectral energy, as seen in Table 4.

3.2.3 Oscillations of 2–4-year periods

The South and North Pacific are the basins presenting the highest correlation values with the global mean SST energy for the 2–4-year spectral range, 0.86 and 0.91, respectively, similar to the 1–2-year spectral range energy previously shown. This strong association indicates that the global energy, relatively to the 2–4-year oscillations, is mostly defined by the Pacific basins (Latif and Barnett 1994; Gu and Philander 1997). During the whole period, 1884–2014, we detect three large subperiods characterized by multidecadal variability, as shown in Fig. 8: 1884–1895 and 1964–2014, marked by higher energy, and 1906–1963, marked by lower energy (SST variance values are displayed as an anomaly for easier visualization).

It is interesting to note that the 2–4-year spectral range SST variance in the North and South Pacific basins, between 1906 and 1963—the middle of the whole period—presents minimum values (1926–1936 and 1944–1954), while that associated with the Indian basin presents maximum values (Fig. 8). This aspect suggests that the Pacific and Indian Oceans present, for specific spectral ranges and periods, inverted signals in terms of SST energy. From 1960 until the present, the strong inverted signal in these two basins (Pacific and Indian) has no longer been observed, and they still present the same signal for

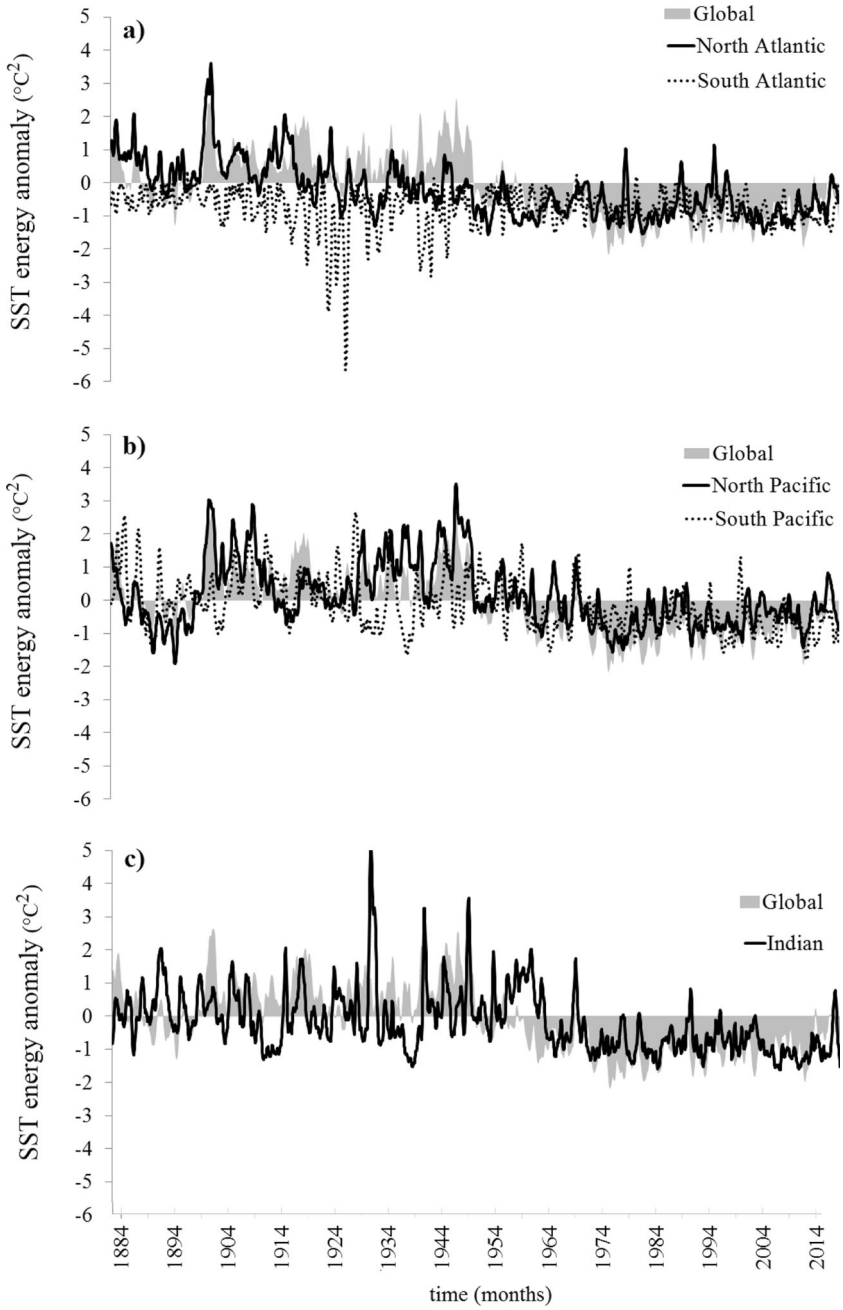

Fig. 5 Mean SST variance for the 1–12-month spectral range for global mean (gray bars): **a** North (continuous black line) and South (dotted black line) Atlantic, **b** North (continuous black line) and South (dotted black line) Pacific, and **c** Indian (continuous black line) basins, in the 1884–2014 period

Table 1 Linear correlation between the global mean and oceanic basins 1–12-month spectral range SST variance, for the period 1884–2014. All the values present statistical significance at the $p = 0.025$ (Student's t test)

	1884–2014	1884–1949	1950–2014
North Atlantic	0.49	0.48	0.30
North Pacific	0.75	0.70	0.76
Indian	0.56	0.30	0.65
South Pacific	0.55	0.50	0.60
South Atlantic	0.64	0.18	0.72

the last two peaks (after 1993). The changes after the 1960s and 1970s (Setoh et al. 1999; An and Wang 2000; Wang and An 2001) are also associated with changes in ENSO patterns (Wang and An 2001; Kleeman et al. 1999; Fedorov and Philander 2000) and, as a consequence, in the subtropical thermocline (Gu and Philander 1995) and atmospheric circulation patterns (Kleeman et al. 1999; Fedorov and Philander 2000; An and Wang 2000; Wang and An 2001). The increase in the global SST variance after the 1970s is another important aspect seen in Fig. 8. Based on the multivariate ENSO index (MEI), Lee et al. (2012) also identified changes in the SST signal after the 1970s. McPhaden et al. (2006) and Mantua

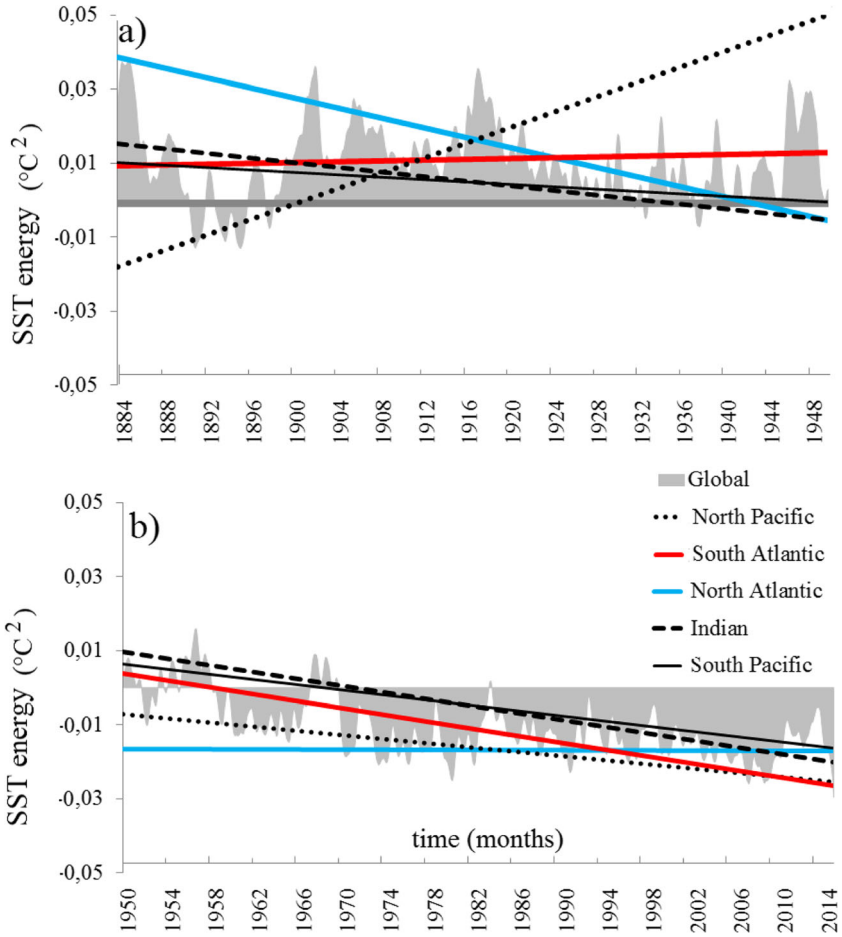

Fig. 6 **a** Global mean SST variance (gray bars) for the 1–12-month spectral range between 1884 and 1949 and linear trends for oceanic basins. The linear trends refer to SST variance averages of North (blue line) and South Atlantic (red line), North (dotted black line) and South Pacific (continuous black line), and Indian (dashed line) basins. **b** Idem to **a**, but for the 1950–2014 period

and Hare (2002) associated the changes in the ENSO evolution in the 1970s with the characteristic PDO timescale. Wang and An (2001), using an ocean-atmosphere coupled model, showed the association between the changes in the SST signal in the 1970s, the wind pattern and dynamics changes in the surface oceanic layer in Pacific areas.

The temporal similarity observed between global SST variance for the 2–4-year spectral range (Fig. 8) and that related to the North and South Pacific basins for the whole period (showing linear correlation of $r = 0.86$ and $r = 0.91$, respectively) and also for the particular EN periods 1972–1973 ($r > 0.99$), 1982–1983 ($r > 0.95$), and 1997–1998 ($r > 0.88$) indicates how the Pacific Ocean is important in the global mean specifically for this oscillation scale (correlation values are indicated in Table 5). The Atlantic and Indian basins present low correlation values for the whole period, and although some high correlation values are observed for specific EN events, no persistence is observed in the signal (Table 5). The period between 1964 and 2014 is marked by high SST variance values of the 2–4-year spectral range over North and South Pacific concomitantly with strong EN events 1972–1973, 1982–1983, and 1997–1998 (Fig. 8) corroborating the results of various authors (Jin et al. 2001, 2003; An and Jin 2004; Wang and Picaut 2004; Okumura and Deser 2010).

Table 2 Idem to Table 1, but for the 1–2-year spectral range. Values marked by (*) present statistical significance at $p = 0.05$ (Student's t test)

	1884–2014	1884–1949	1950–2014
North Atlantic	− 0.04	0.20*	− 0.22*
North Pacific	0.73*	0.57*	0.85*
Indian	0.16*	0.28*	− 0.02
South Pacific	0.80*	0.74*	0.85*
South Atlantic	0.05	0.08	− 0.06

3.2.4 Oscillations of 4–8-year periods

As in the previous spectral ranges analysis, oscillations of 4–8 years are also considered for the whole period, 1884–2014. Physically, this spectral range is closely associated to low-frequency ENSO phenomena (McPhaden 2002). In recent studies, An and Wang (2000) and Wang and An (2001) characterize the main ENSO variability in the range of 4–6 years, while Torrence and Webster's (1999) previous studies characterize them in the range of 2–7 years. ENSO is considered the most important tropical mode able to influence the atmosphere

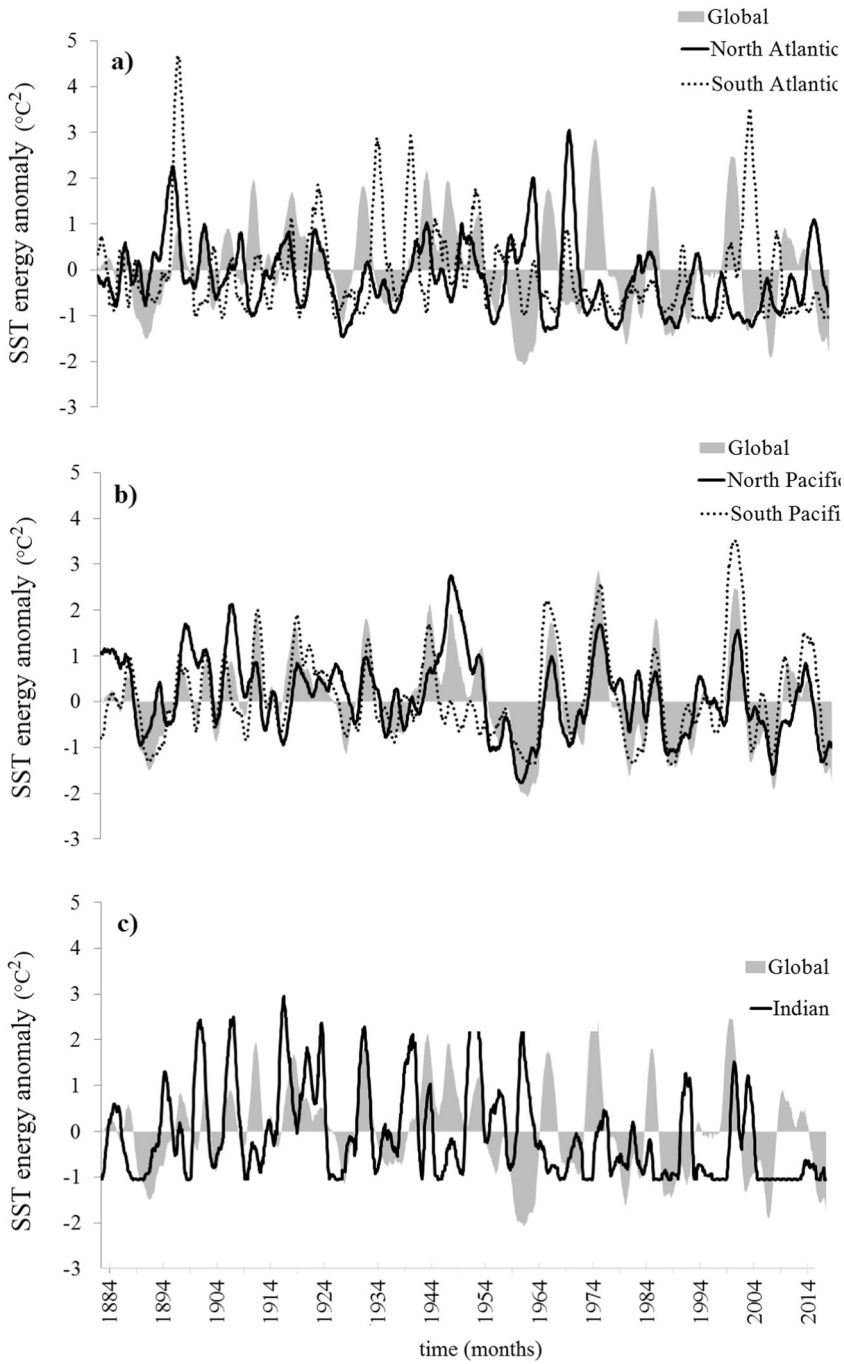

Fig. 7 Mean SST variance for the 1–2-year spectral range for global mean (gray bars): **a** North (continuous black line) and South (dotted black line) Atlantic, **b** North (continuous black line) and South (dotted black line) Pacific, and **c** Indian (continuous black line) basins, in the 1884–2014 period

Table 3 Linear correlation coefficient between the global SST variance for the 1–2-year spectral range and mean values for the North and South Pacific, North and South Atlantic, and Indian basins. Correlation values for specific El Niño (1965–1966; 1972–1973; 1982–1983; 1997–1998) and La Niña (1970–1971 and 1988–1989) events are in italics and bold, respectively. (*) identifies significant statistical values for $p = 0.05$

	1884–1949	1950–2014	*1965/1966*	*1972/1973*	*1982/1983*	*1997/1998*	**1970/1971**	**1988/1989**
North Atlantic	0.20*	− 0.22*	*− 0.85**	*0.26*	*0.20*	*− 0.18*	**− 0.80***	**− 0.66***
South Atlantic	0.07	− 0.06	*− 0.40*	*− 0.82**	*0.76**	*0.47**	**− 0.01**	**0.90***
Indian	0.29*	− 0.02	*− 0.72**	*− 0.26*	*0.45*	*− 0.32*	**− 0.85***	**− 0.51***
North Pacific	0.57*	0.85*	*0.99**	*0.78**	*0.96**	*0.62**	**0.98***	**− 0.56***
South Pacific	0.74*	0.85*	*0.99**	*0.70**	*0.96**	*0.96**	**0.99***	**0.17**

Table 4 Linear correlation coefficient between the SST anomalies over the equatorial Pacific and the SST variance of the 1–12-month, 1–2-year, 2–4–year, and 4–8-year spectral ranges, separately for El Niño and La Niña periods observed from 1950 to 2010. Statistically significant values at $p = 0.01$ (Student's t test) are marked by (*)

La Niña	El Niño	Freq1-12mo	Freq1-2yr	Freq2-4yr	Freq4-8yr
Jan/1950–Mar/1951		0.16	0.75*	0.71*	0.74*
Apr/1954–Jan/1957		0.30	− 0.59	0.62*	− 0.14
	Apr/1957–Jul/1958	0.60	0.67*	0.67*	0.57
Apr/1964–Jan/1965		− 0.56	0.60	0.53	− 0.63*
	Jun/1966–Apr/1966	− 0.37	0.84	− 0.78	0.69
	Nov/1966–Jan/1970	0.75	− 0.42	0.70*	− 0.49
Jul/1970–Jan/1972		− 0.43	0.64	0.40	0.38
	May/1972–Mar/1973	0.66	− 0.36	0.714*	− 0.46
May/1973–May/1975		0.37	− 0.43	− 0.45*	0.41
	Sep/1976–Feb/1977	0.87*	0.90*	0.89*	− 0.57
	Oct/1977–Jan/1978	0.89*	− 0.72*	0.80*	0.46
	May/1982–Jun/1983	0.91*	0.94*	0.89*	0.94*
Oct/1984–Sep/1985		− 0.60	0.80*	0.76	0.40
	Aug/1986–Feb/1988	− 0.69	0.35	− 0.57	0.97*
May/1988–May/1989		0.76*	− 0.71*	− 0.76*	− 0.73*
	May/1991–Jul/1992	0.61*	0.47	− 0.56	0.45
	May/1994–Mar/1995	0.82*	− 0.65	0.67	0.73
	May/1997–May/1998	− 0.05	0.40	0.63*	− 0.27
Jul/1998–Feb/2001		0.03	0.64*	0.45	0.37
	May/2002–Mar/2008	− 0.4	0.39	− 0.28	− 0.12
	Jun/2004–Feb/2005	0.26	− 0.45	0.04	− 0.31
	Aug/2005–Fev/2006	0.82*	0.73	0.48	− 0.73
Sep/2007–May/2008		0.36	− 0.78*	0.73	0.01

at mid and high latitudes (Bjerknes 1969; Gershunov and Barnett 1998), in addition to tropical areas. This aspect makes the extratropical atmosphere more barotropic equivalent (Hoskins et al. 1977; Hoskins and Karoly 1981; Hendon and Hartmann 1982; Kasahara and Silva Dias 1986), providing more climatic complexity to these latitudes.

A global mean of SST variance in the spectral range of 4–8 years presents periods of low (1921–1935, 1961–1981, and 2002–2014) and high (1910–1921, 1935–1961, and 1983–2001) values, as seen in Figs. 2 and 9. Low and high values of SST variance for this spectral range can be characterized by two main aspects: firstly, the concomitance of maximum and minimum values with ENSO episodes (EN: 1918–1919, 1939–1941, 1953, 1982–1983, 1997–1998 and LN: 1928–1929, 1973–1976, 2007–2008) and, secondly, the important role of Pacific basins (dotted and continuous lines in Fig. 9) in the global mean. North Atlantic SST variance (red line in Fig. 9) maintains some linear similarity with the global mean ($r = 0.56$), as shown in Table 6, the first half period being much more linearly correlated than the second half of the period.

The North and South Pacific present linear correlation values of 0.84 and 0.87 with the global mean, respectively, shown in Fig. 9 and Table 6. Since the North Atlantic shows linear correlation equal to 0.56 (Table 6) with the global mean, it suggests some association with Pacific basins ($r = 0.56$ for the North Pacific). Actually, the North Atlantic SST variance for the 4–8-year spectral range is out of phase (somewhat delayed) in relation to the energy observed in North and South Pacific for the same scale (Fig. 9).

In relation to the ENSO occurrence, the SST variance for the 4–8-year spectral range over the Pacific basins presents a particular aspect if compared to the other ranges: the maximum values are in all cases associated with EN, as indicated in Fig. 9, especially allowing the identification of the time when the spectral energy begins to increase some months or years before the peak. EN events occur in association with the highest energy values. The strong EN events occurring in the 1915–1916, 1940–1942, 1955–1956, 1982–1983, and 1997–1998 periods are inserted into subperiods for which the SST variance of 4–8 years had begun to rise for earlier months, as seen in Fig. 9. This aspect suggests that the energy associated with the SST variance for the 4–8-year spectral range can be considered a potential predictor for EN occurrence. These results corroborate those highlighted by Kestin et al. (1998), where stochastic simulations for low-frequency data were used for ENSO forecasts.

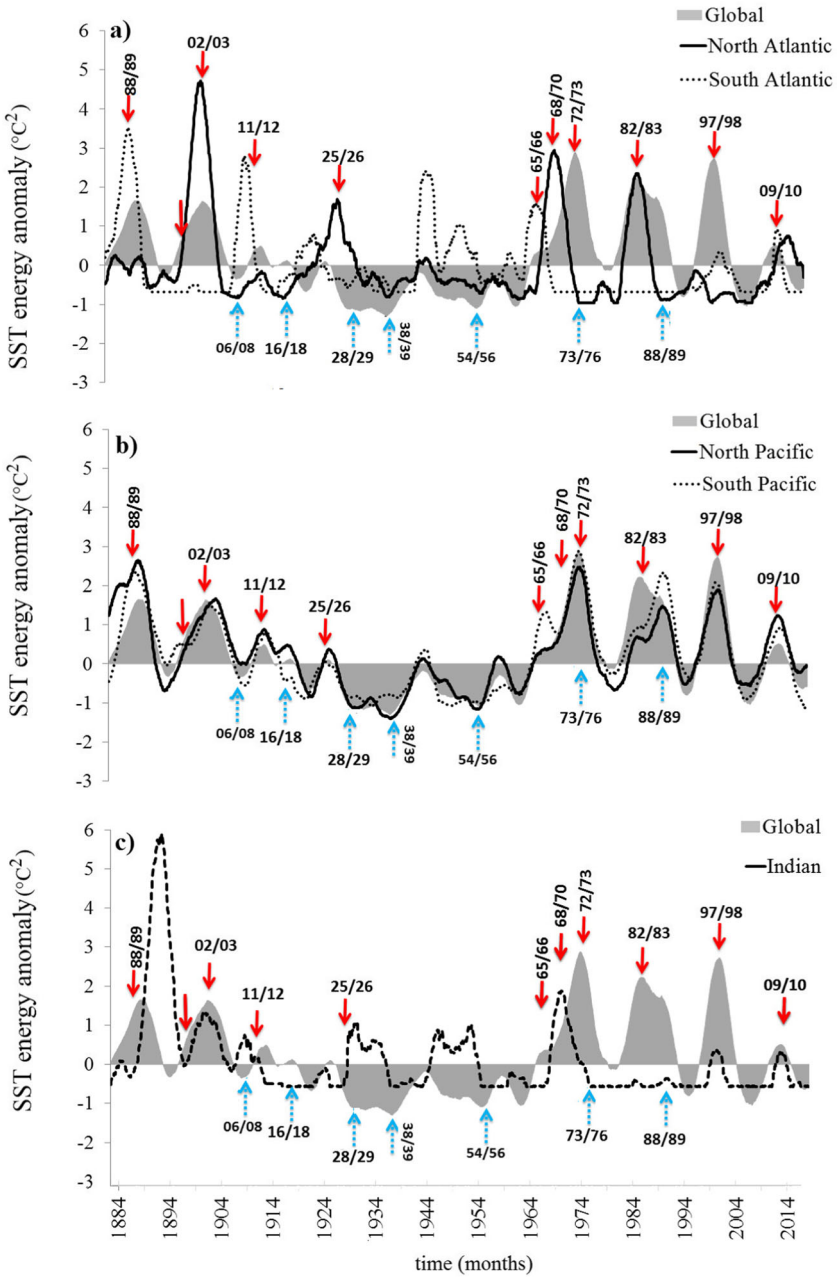

Fig. 8 Idem to Fig. 5, but for the 2–4-year spectral range energy

Another important point is the long duration of high SST variance values for the 4–8-year spectral range in the recent period of 1980–2001, being associated with multiple EN episodes, as also pointed out in the Cane and Zebiak (1985) theory. During this same period (1980–2001), maximum SST variance values for the 4–8-year oscillations were associated with two strong EN events, 1982–1983 and 1997–1998. On the other hand, minimum SST variance values for

Table 5 Idem to Table 3 but for the 2–4-year spectral range

	1884–2014	1972/1973	1982/1983	1997/1998	**1970/1971**	**1988/1989**
North Atlantic	0.35*	*0.71**	*0.98**	*− 0.74*	**− 0.99***	**0.12**
South Atlantic	− 0.04	*0.30*	*− 0.34*	*0.02*	**− 0.20**	**0.28**
Indian	0.12*	*0.99**	*− 0.49*	*0.52**	**− 0.99***	**0.94***
North Pacific	0.87*	*0.99**	*0.95**	*0.96**	**0.99***	**0.99***
South Pacific	0.92*	*0.99**	*0.97**	*0.88**	**0.99***	**0.99***

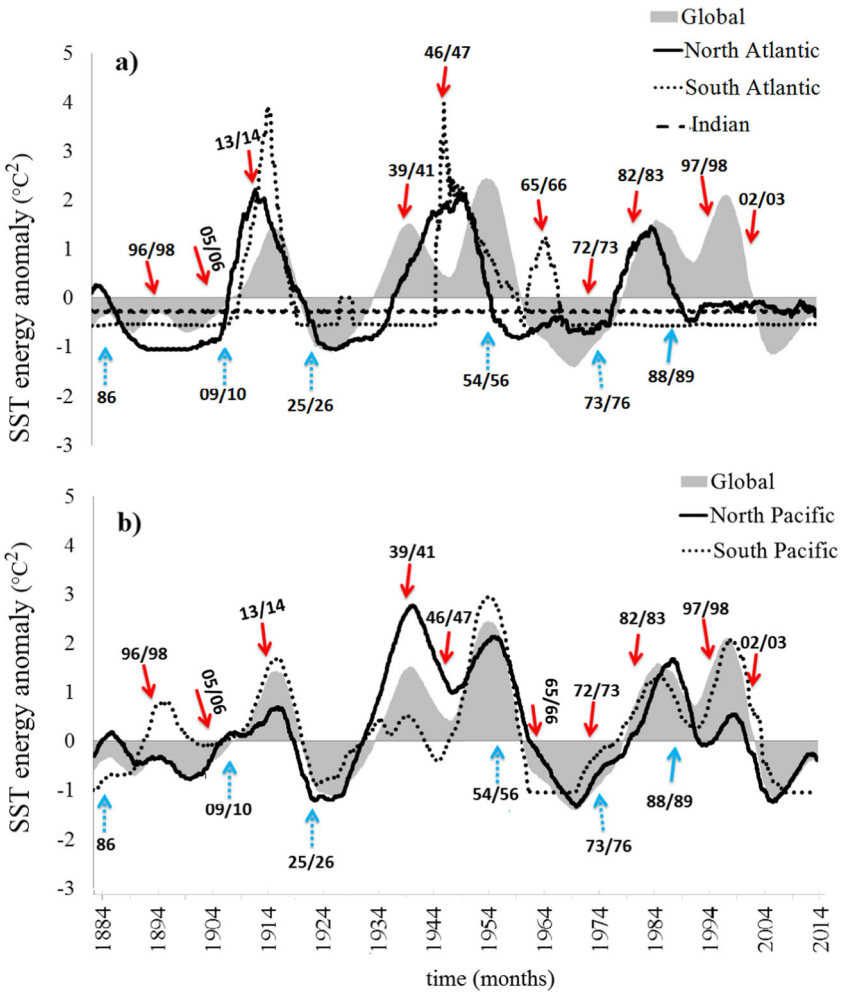

Fig. 9 Idem to Fig. 5, but for the 4–8-year spectral range

this spectral range (4–8 years) in the 1980–2001 period were associated with strong LN events. In Fig. 9, we can see a considerable minimum SST variance between strong EN events, which must be associated with the 1988–1989 LN event.

Considering multiple EN events, Cane and Zebiak (1985), Cane et al. (1986), and Wyrtki (1986) have suggested, following theoretical assumptions, that the occurrence of a very strong EN episode following previous warm events can be explained by a gradual thermocline shallowing into equatorial latitudes in the central-west Pacific through Kelvin waves propagation, promoting the transport of a large amount of heat to the eastern Pacific areas. This theoretical assumption can possibly be observed for the 1935–1961 and 1981–2002 periods (Fig. 9), resulting in the respective occurrence of strong EN events in 1957–1959 and 1997–1998. The increase of SST variance in the 4–8-year spectral range associated with the 1982–1983 and 1997–1998 EN events begins in 1975, 13 years before the 1982–1983 event, and it began to decline after 2002. Between 1975 and 2002, the Pacific basins are those that present the highest linear association with the global mean for the 4–8-year spectral range SST variance ($r > 0.88$, Table 6), strengthening their importance in the global mean.

Table 6 Idem to Table 3 but for the 4–8-year spectral range

	1884–2014	1884–1949	1950–2014	*1910/1921*	*1935/1961*	*1981/2002*	**1921/1935**	**1961/1981**	**2002/2014**
North Atlantic	0.56*	0.75*	0.48*	*0.28*	*− 0.03*	*0.03*	**0.67***	**0.82***	**0.34**
South Atlantic	0.31*	0.48*	0.25*	*0.76**	*0.04*	*0.01*	**− 0.23**	**− 0.09**	**− 0.03**
Indian	− 0.03	− 0.01	− 0.05	*0.01*	*0.00*	*− 0.01*	**0.03**	**− 0.08**	**0.02**
North Pacific	0.83*	0.86*	0.88*	*0.86**	*0.67**	*0.48**	**0.77***	**0.84***	**0.09***
South Pacific	0.87*	0.67*	0.94*	*0.99**	*0.86**	*0.85**	**0.89***	**0.76***	**0.53***

In general, Pacific basins are the oceanic areas that mostly contribute to the global mean for the 4–8-year spectral range. This can be seen in the high correlation values computed for low (data in bold, Table 6) and high (data in italics, Table 6) SST variance values, as shown in Table 6. The North Atlantic basin also seems to play an important role in the global mean, particularly for periods of low SST variance values (data in bold in Table 6) when linear correlation values are higher.

3.2.5 Oscillations of 8–12-year periods

The SST variability for the 8–12-year periods presents low absolute values when compared with the other spectral ranges, which can be seen in Fig. 2b. Higher energy values in the 8–12-year spectral ranges are observed in the 1884–1888 and 1990–2007 periods, except in short periods around 1903 and 1920. The strong EN event in 1997–1998 occurred during the second period of high 8–12-year oscillation SST energy values, 1990–2007, which presents maximum values close to 1998. The 1997–1998 EN closely relates to the spectral energy ranges of 4–8 and 8–12 years and does not seem to be associated with the higher frequency spectral ranges (1–12 months, 1–2 years, and 2–4 years) (Figs. 5, 6, and 7). Other prior EN events observed in the time series can be associated with higher frequency oscillations (e.g., the 1902–1903 and 1918–1919 EN events are closely associated with the 1–12- and 1–2-year (only for the second case) spectral range); the 1990–1993 EN is associated with the 4–8-year spectral range. It is suggested that the association with lower frequency can partially explain the strong intensity of the 1997–1998 EN.

In the 1990s, the time between the minimum (close to 1991) and maximum (close to 1997–1998) SST variance values is equal to 6 years (Fig. 2b). After the maximum values reached in this period (1997–1998), the 8–12-year energy took more 10 years to reach the next minimum values, which happened near to 2007. The precedence of low-frequency oscillations thus characterizes its predictability, with a lack of an adequate energy limit to provide an efficient predictor.

4 Conclusions

In this study, the wavelet technique was applied to the global monthly SST from the dataset of Kaplan et al. (1998) (with resolution of 2.5°) in order to better understand the temporal and spatial patterns of SST energy associated with oscillations characterized by periodicities of 1–12 months and 1–2, 2–4, 4–8, and 8–12 years, in the 1884–2014 period. Although satellite data began to be used in numerical models after 1978 (Brasnett 2008), wavelet analysis applied to SST data does not show any obvious change from before to after this date.

The wavelet analysis applied for gridded SST distributed over the globe allowed the observation of the spatial evolution of the energy associated with each selected spectral range throughout the period. This process led to a more accurate identification of more and less energetic areas and periods within the dataset. The dynamic evolution of SST energy in the selected timescales, throughout the study period, is shown in videos hosted at the http://krlosbatist.wixsite.com/meusite, while this paper presents only mean results over distinct spatial domains.

Results obtained for large areas (tropical, subtropical, and extratropical latitudes) show more important oscillation periodicities in tropical areas of close to 4 years, while extratropical areas show importance at higher periodicities. Thus, the first results suggest that oceanic tropical phenomena are much more strongly driven by intraseasonal and interannual oscillations, which is corroborated by previous references (An and Wang 2000; Wang and An 2001; Raupp and Silva Dias 2006; Setoh et al. 1999; Torrence and Compo 1998; Torrence and Webster 1999; Saji et al. 1999) than extratropical phenomena, which are more associated with decadal and multidecadal scales, also mentioned by other authors (Latif and Barnett 1994 and Gu and Philander 1997).

The most important result obtained from the temporal analysis between distinct spectral ranges, during the period 1884–2014, is the decreasing of energy for high-frequency oscillations (1–12 months, 1–2 years, and 2–4 years) in relation to low-frequency oscillations (4–8 and 8–12 years), which, instead, show increasing values during the period under study. Physically, it means that higher and lower oscillation phenomena at the oceanic surface have exchanged energy with each other, with higher frequency phenomena losing energy to lower frequency phenomena. This aspect is also mentioned in theoretical studies, such as those of Raupp and Silva Dias (2006) and Ramirez et al. (2017), where the energy exchange between tropical convection and ENSO phenomena plays a critical role as a controlling mechanism. The highest spectral energy decrease is mainly observed in the North and South Atlantic basins, while the largest increase is observed in North and South Pacific.

For the equatorial Pacific, the results show that the ENSO phenomena have changed their characteristic energy scale over time, from the 2–4- to the 4–6-year spectral range, while those associated with the 1–2-year oscillations had their energy weakened. This aspect of ENSO changes is in agreement with the results shown by An and Wang (2000), Setoh et al. (1999), and Rasmusson et al. (1990) and is associated with the energy loss transfer from faster to slower phenomena.

The North and South Pacific are the basins which are more closely linearly correlated with the global mean for all considered spectral ranges in this study, which means that these basins present the major part of the global energy and better represent it. This aspect is especially important for the energy related to the spectral ranges of 2–4 and 4–8 years, which show the highest correlation values with the global mean.

For the 2–4-year oscillations, the linear correlations between the global and North and South Pacific were 0.87 and 0.92, respectively. For the 4–8-year oscillations, the linear correlations with North and South Pacific were 0.84 and 0.87, respectively. The spectral range of 1–2 years shows slightly lower linear correlations for the North and South Pacific basins (0.73 and 0.79, respectively). The SST energy related to the spectral range of 4–8 years, in the North Atlantic basin, also shows an important correlation with the global mean (r = 0.56), but not so high as that of the Pacific basins. The Atlantic and Indian Oceans show lower correlation values with the global mean. Considering isolated ENSO events (both for EN and LN), the 1–2-year oscillation energy is the spectral energy most correlated with the global mean. Although the SST variance values in each oceanic basin have been considered as a spatial average in this study, it is important to take into account the relative importance of each oceanic basin by considering the respective basin size in further studies.

Another important result is the ENSO predictability through the time evolution analysis of lower frequency oscillations, especially in the case of 4–8-year SST energy, in which the energy increase begins 3–5 years earlier and ends up to 5 years after the EN maximum. This aspect can clearly be seen in the EN events of 1939–1941, 1957–1959, 1982–1983, and 1997–1998. Although the results obtained in this study were based on SST values averaged over extended areas (oceanic basins), analogous results can be reproduced in smaller and specific regions, improving the predictability of the signal. The 8–12-year SST energy oscillation also contains information important for longer period predictability studies.

Acknowledgments The authors of this paper would like to thank NOAA/OAR/ESRL PSD, Boulder, Colorado, USA, for making available the Kaplan SST V2 data from their web site at http://www.esrl.noaa.gov/psd/. They would also like to thank Christopher Torrence and Gilbert P. Compo for making available the original scripts of the wavelets technique made available for public use at http://paos.colorado.edu/research/wavelets/. They are also grateful to the postgraduate program in Physical Geography of the University of São Paulo, Brazil, which provided the technical support for the research and development.

Funding information The first (Carlos Batista Silva) and second (Maria Elisa Siqueira Silva) authors acknowledge the support of CAPES which provided the doctorate scholarship and the financial support received from CNPq, CAPES, and FAPESP (Proc. No. 08/58010-9; 2017/09308-9). Pedro L. Silva Dias acknowledges the support of CNPq, under grant 309395/2013-5, FAPESP project PACMEDY No. 2015/50686-1 and CAPES project PALEOCEAN. TA also acknowledges the support of CNPq, under grants 304298/2014-0 and 401155/2014-5.

References

An SI, Jin FF (2004) Nonlinearity and asymmetry of ENSO. J Clim 17(12):2399–2412. https://doi.org/10.1175/1520-0442(2004)017<2399:NAAOE>2.0.CO;2

An SI, Wang B (2000) Interdecadal change of the structure of the ENSO mode and its impact on the ENSO frequency. J Clim 13(12):2044–2055. https://doi.org/10.1175/1520-0442(2000)013<2044:ICOTSO>2.0.CO;2

Andreoli RV, Kayano MT (2004) Multi-scale variability of the sea surface temperature in the Tropical Atlantic. J Geophys Res Oceans 109. https://doi.org/10.1029/2003JC002220

Bjerknes J (1969) Atmospheric teleconnections from the Equatorial Pacific. Mon Weather Rev 97:163–172. https://doi.org/10.1175/1520-0493(1969)097<0163:ATFTEP>2.3.CO;2

Brasnett B (2008) The impact of satellite retrievals in a global sea-surface-temperature analysis. Q J R Meteorol Soc 134(636):1745–1760. https://doi.org/10.1002/qj.319

Cane MA, Zebiak SE (1985) A theory for El Nino and the Southern Oscillation. Science 228(4703):1085–1087. https://doi.org/10.1126/science.228.4703.1085

Cane MA, Zebiak SE, Dolan SC (1986) Experimental forecasts of El Niño. Nature 321:827–832. https://doi.org/10.1038/321827a0

Carton JA, Cao X, Giese BS, Da Silva AM (1996) Decadal and interannual SST variability in the tropical Atlantic Ocean. J Phys Oceanogr 26(7):1165–1175. https://doi.org/10.1175/1520-0485(1996)026<1165:DAISVI>2.0.CO;2

Chu JE, Ha KJ, Lee JY, Wang B, Kim BH, Chung CE (2014) Future change of the Indian Ocean basin-wide and dipole modes in the CMIP5. Clim Dyn 43(1 a 2):535–551

Davis RE (1976) Predictability of sea surface temperature and sea level pressure anomalies over the North Pacific Ocean. J Phys Oceanogr 6(3):249–266. https://doi.org/10.1175/1520-0485(1976)006<0249:POSSTA>2.0.CO;2

Daubechies I (1990) The wavelet transform time-frequency localization and signal analysis. IEEE Trans Inf Theory 36:961–1004. https://doi.org/10.1109/18.57199

Farge M (1992) Wavelet transforms and their applications to turbulence. J Atmos Sci, Palo Alto 24:395–457

Fedorov AV, Philander SG (2000) Is El Niño changing? Science 288(5473):1997–2002. https://doi.org/10.1126/science.288.5473.1997

Flandrin P (1988) Time-frequency and timescale. IEEE Fourth Annu. ASSP Workshop Spectrum Estimation and Modeling, Minneapolis, August 1988, pp 77–80

Francis RC, Hare HS (1994) Decadal-scale regime shifts in the large marine ecosystems of the Northeast Pacific: a case for historical science. Fish Oceanogr 3:279–291. https://doi.org/10.1111/j.1365-2419.1994.tb00105.x

Gershunov A, Barnett TP (1998) Interdecadal modulation of ENSO teleconnections. Bull Am Meteorol Soc 79(12):2715–2725. https://doi.org/10.1175/1520-0477(1998)079<2715:IMOET>2.0.CO;2

Gu D, Philander S (1995) Secular changes of annual and interannual variability in the tropics during the past century. J Clim 8:864–876. https://doi.org/10.1175/1520-0442(1995)008<0864:SCOAAI>2.0.CO;2

Gu D, Philander SG (1997) Interdecadal climate fluctuations that depend on exchanges between the tropics and extratropics. Science 275(5301):805–807. https://doi.org/10.1126/science.275.5301.805

Hare SR, Francis RC (1995) Climate change and salmon production in the Northeast Pacific Ocean. Canadian Special Publication of Fisheries and Aquatic Sciences 357–372

Hendon HH, Hartmann DL (1982) Stationary waves on a sphere: sensitivity to thermal feedback. J Atmos Sci 39(9):1906–1920. https://doi.org/10.1175/1520-0469(1982)039<1906:SWOASS>2.0.CO;2

Horel JD, Wallace JM (1981) Planetary scale atmospheric phenomena associated with the Southern Oscillation. Mon Weather Rev 109:813–829. https://doi.org/10.1175/1520-0493(1981)109<0813:PSAPAW>2.0.CO;2

Hoskins BJ, Karoly DL (1981) The steady linear response of a spherical atmosphere to thermal and orographic forcing. J Atmos Sci 38:

1179–1196. https://doi.org/10.1175/1520-0469(1981)038<1179:TSLROA>2.0.CO;2

Hoskins BJ, Simmons AJ, Andrews DG (1977) Energy dispersion in a barotropic atmosphere. Q J R Meteorol Soc 103(438):553–567. https://doi.org/10.1002/qj.49710343802

Huang B, Banzon VF, Freeman E, Lawrimore J, Liu W, Peterson TC, Zhang HM et al (2015) Extended reconstructed sea surface temperature version 4 (ERSST. v4). Part I: upgrades and intercomparisons. J Clim 28(3):911–930. https://doi.org/10.1175/JCLI-D-14-00006.1

Janicke H, Böttinger M, Mikolajewicz U, Scheuermann G (2009) Visual exploration of climate variability changes using wavelet Analysis. IEEE Transactions on Visualization and Computer Graphics. v 15, 6, nov-dec. 1375–1382. https://doi.org/10.1109/TVCG.2009.197

Jin FF, Hu ZZ, Latif M, Bengsson L, Roeckner E (2001) Dynamical and cloud-radiation feedbacks in El Niño and greenhouse warming. Geophys Res Lett 28:1539–1542. https://doi.org/10.1029/2000GL012078

Jin FF, An SI, Timmermann A, Zhao J (2003) Strong El Niño events and nonlinear dynamical heating. Geophys Res Lett 30:1120. https://doi.org/10.1029/2002GL016356

Kaplan A, Cane MA, Kushnir AC, Benno CM, Rajagoplan BB (1998) Analyses of global sea surface temperature 1856–1991. J Geophys Res 103:18567–18589. https://doi.org/10.1029/97JC1736

Karoly DJ (1989) Southern hemisphere circulation features associated with El Niño-Southern Oscillation events. J Clim 2:1239–1252. https://doi.org/10.1175/1520-0442(1989)002<1239:SHCFAW>2.0.CO;2

Kasahara A, Silva Dias PL (1986) Response of planetary waves to stationary tropical heating in a global atmosphere with meridional and vertical shear. J Atmos Sci 43(18):1893–1912. https://doi.org/10.1175/1520-0469(1986)043<1893:ROPWTS>2.0.CO;2

Kayano MT, Andreoli RV (2004) Decadal variability of northern Northeast Brazil rainfall and its relation to tropical sea surface temperature and global sea level pressure anomalies. J Geophys Res Oceans 109(C11). https://doi.org/10.1029/2004JC002429

Kestin TS, Karoly DJ, Yano JI, Rayner NA (1998) Time-frequency variability of ENSO and stochastic simulations. J Clim 11(9):2258–2272. https://doi.org/10.1175/1520-0442(1998)011<2258:TFVOEA>2.0.CO;2

Kleeman R, McCreary JP, Klinger BA (1999) A mechanism for generating ENSO decadal variability. Geophys Res Lett 26(12):1743–1746. https://doi.org/10.1029/1999GL900352

Kumar P, Foufoula-Georgoiu E (1997) Wavelets analysis for geophysical applications. Rev Geophys 35(4):385–412. https://doi.org/10.1029/97RG00427

Latif M, Barnett TP (1994) Causes of decadal climate variability over the North Pacific and North America. Science 266(5185):634–637. https://doi.org/10.1126/science.266.5185.634

Latif M, Barnett TP (1995) Interactions of the tropical oceans. J Clim 8(4):952–964. https://doi.org/10.1175/1520-0442(1995)008<0952:IOTTO>2.0.CO;2

Latif M, Barnett TP (1996) Decadal climate variability over the North Pacific and North America: Dynamics and predictability. J Clim 9(10):2407–2423. https://doi.org/10.1175/1520-0442(1996)009<2407:DCVOTN>2.0.CO;2

Lau KM, Weng H (1995) Climate signal detection using wavelet transform: How to make a time series sing. Bull Am Meteorol Soc 76(12):2391–2402. https://doi.org/10.1175/1520-0477(1995)076<2391:CSDUWT>2.0.CO;2

Lee HS, Yamashita T, Mishima T (2012) Multi-decadal variations of ENSO, the Pacific Decadal Oscillation and tropical cyclones in the western North Pacific. Prog Oceanogr 105:67–80. https://doi.org/10.1016/j.pocean.2012.04.009

Mak M (1995) Orthogonal wavelet analysis: interannual variability in the sea surface temperature. Bull Am Meteorol Soc 76(11):2179–2186. https://doi.org/10.1175/1520-0477(1995)076<2179:OWAIVI>2.0.CO;2

Mantua NJ, Hare SR (2002) The Pacific Decadal Oscillation. J Oceanogr 58:35–44. https://doi.org/10.1023/A:1015820616384

Mantua NJ, Hare SR, Zhang Y, Wallace JM, Francis RC (1997) A Pacific interdecadal climate oscillation with impacts on salmon production. Bull Am Meteorol Soc 78:1069–1079. https://doi.org/10.1175/15200477

McPhaden MJ (2002) El Niño and La Niña: causes and global consequences. In: Encyclopedia of global environmental change. Wiley, Chichester, pp 353–370

McPhaden MJ, Zebiak SE, Glantz MH (2006) ENSO as an integrating concept in earth science. Science 314(5806):1740–1745. https://doi.org/10.1126/science.1132588

Minobe S (1997) A 50-70 year climatic oscillation over the North Pacific and North America. Geophys Res Lett 24 (6):683–686. https://doi.org/10.1029/97GL00504

Minobe S, Manabe T, Shouji A (2002) Maximal wavelet filter and its application to bidecadal oscillation over the Northern Hemisphere through the twentieth century. J Clim 15(9):1064–1075. https://doi.org/10.1175/1520-0442(2002)015<1064:MWFAIA>2.0.CO;2

Morlet J (1983) Sampling theory and wave propagation. In: Issues in acoustic signal—image processing and recognition. Springer, Berlin, pp 233–261. https://doi.org/10.1007/978-3-642-82002-1_12

Newman M, Compo GP, Alexander MA (2003) ENSO-forced variability of the Pacific decadal oscillation. J Clim 16(23):3853–3857. https://doi.org/10.1175/1520-0442(2003)016<3853:EVOTPD>2.0.CO;2

Nobre P, Shukla J (1996) Variations of sea surface temperature, wind stress, and rainfall over the tropical Atlantic and South America. J Clim 9(10):2464–2479. https://doi.org/10.1175/1520-0442(2003)016<3853:EVOTPD>2.0.CO;2

Okumura YM, Deser C (2010) Asymmetry in the duration of El Niño and La Niña. J Clim 23(21):5826–5843. https://doi.org/10.1175/2010JCLI3592.1

Ramirez E, Silva Dias PL, Raupp CF (2017) Multiscale atmosphere-ocean interactions and the low frequency variability in the equatorial region. J Atmos Sci 74:2503–2523. https://doi.org/10.1175/JAS-D-15-0325.1

Rasmusson EM, Wang X, Ropelewski CF (1990) The biennial component of ENSO variability. J Mar Syst 1(1–2):71–96. https://doi.org/10.1016/0924-7963(90)90153-2

Raupp CF, Silva Dias PL (2006) Dynamics of resonantly interacting equatorial waves. Tellus A 58(2):263–279. https://doi.org/10.1111/j.1600-0870.2006.00151.x

Saji NH, Yamagata T (2003) Structure of SST and surface wind variability during Indian Ocean dipole mode events: COADS observations. J Clim 16:2735–2751. https://doi.org/10.1175/1520-0442(2003)016<2735:SOSASW>2.0.CO;2

Saji NH, Goswami BN, Vinayachandran PN, Yamagata T (1999) A dipole mode in the tropical Indian Ocean. Nature 401(6751):360–363. https://doi.org/10.1038/43854

Setoh T, Imawaki S, Ostrovskii A, Umatani SI (1999) Interdecadal variations of ENSO signals and annual cycles revealed by wavelet analysis. J Oceanogr 55(3):385–394. https://doi.org/10.1023/A:1007854415983

Torrence C, Compo GP (1998) A practical guide to wavelet analysis. Bull Am Meteorol Soc 79:61–78. https://doi.org/10.1175/1520-0477(1998)079<0061:APGTWA>2.0.CO;2

Torrence C, Webster PJ (1999) Interdecadal changes in the ENSO-monsoon system. J Clim 12(8):2679–2690. https://doi.org/10.1175/1520-0442(1999)012<2679:ICITEM>2.0.CO;2

Troup AJ (1965) The southern oscillation. Q J R Meteorol Soc 91(390):490–506. https://doi.org/10.1002/qj.49709139009

Vitorino MI, Silva Dias PL, Ferreira NJ (2006) Observational study of the seasonality of the submonthly and intraseasonal signal over the

tropics. Meteorog Atmos Phys 93(1–2):17–35. https://doi.org/10.1007/s00703-005-0162-7

Wagner RG (1996) Decadal-scale trends in mechanisms controlling meridional sea surface temperature gradients in the tropical Atlantic. J Geophys Res Oceans 101(C7):16683–16694. https://doi.org/10.1029/96JC01214

Walker GT, Bliss EM (1932) World weather V. Mem Roy Meteor Soc 4:53–84

Wang B, An SI (2001) Why the properties of El Niño changed during the late 1970s. Geophys Res Lett 28(19):3709–3712. https://doi.org/10.1029/2001GL012862

Wang C, Picaut L (2004) Understanding ENSO physics-A review, in Earth Climate: The Ocean-Atmosphere Interaction. Geophys Monogr Ser 147. https://doi.org/10.1029/147GM02

Webster PJ, Moore AM, Loschnigg JP, Leben RR (1999) Coupled ocean–atmosphere dynamics in the Indian Ocean during 1997–98. Nature 401(6751):356–360. https://doi.org/10.1038/43848

Weng HY, Lau KM (1994) Wavelet, period-doubling and time frequency localization with application organization of convection over the tropical western Pacific. J Atmos Sci 51(17):2523–2541. https://doi.org/10.1175/1520-0469(1994)051<2523:WPDATL>2.0.CO;2

Whitcher B, Guttorp P, Percival DB (2000) Wavelet analysis of covariance with application to atmospheric time series. J Geophys Res Atmos (1984–2012) 105(D11):14941–14962. https://doi.org/10.1029/2000JD900110

Wyrtki K (1986) Water displacements in the Pacific and the genesis of El Niño cycles. J Geophys Res 91:7129–7132. https://doi.org/10.1029/JC090iC04p07129

Yamagata T, Behera SK, Rao SA, Guan Z, Ashok K, Saji NH (2003) Comments on "Dipoles, temperature gradient, and tropical climate anomalies". Bull Am Meteorol Soc 84:1418–1422

Zhang Y, Wallace JM, Battisti DS (1997) ENSO-like interdecadal variability: 1900-93. J Clim 10(5):1004–1020. https://doi.org/10.1175/1520-0442(1997)010<1004:ELIV>2.0.CO;2